Stable three-dimensional solitons in attractive Bose-Einstein condensates loaded in an optical lattice

D. Mihalache,[1,2,3] D. Mazilu,[2,3] F. Lederer,[2] B. A. Malomed,[4] L.-C. Crasovan,[1,3] Y. V. Kartashov,[1] and L. Torner[1]

[1]*ICFO-Institut de Ciencies Fotoniques, and Department of Signal Theory and Communications,*
Universitat Politecnica de Catalunya, 08034 Barcelona, Spain

[2]*Institute of Solid State Theory and Theoretical Optics, Friedrich-Schiller Universität Jena, Max-Wien-Platz 1, D-077743 Jena, Germany*

[3]*Horia Hulubei National Institute of Physics and Nuclear Engineering, Department of Theoretical Physics, P.O. Box MG-6,*
Bucharest, Romania

[4]*Department of Interdisciplinary Studies, Faculty of Engineering, Tel Aviv University, Tel Aviv 69978, Israel*

The existence and stability of solitons in Bose-Einstein condensates with attractive interatomic interactions, described by the Gross-Pitaevskii equation with a three-dimensional (3D) periodic potential, are investigated in a systematic form. We find a one-parameter family of stable 3D solitons in a certain interval of values of their norm, provided that the strength of the potential exceeds a threshold value. The minimum number of ^{7}Li atoms in the stable solitons is 60, and the energy of the soliton at the stability threshold is ≈ 6 recoil energies in the lattice. The respective energy versus norm diagram features two cuspidal points, resulting in a typical *swallowtail pattern*, which is a generic feature of 3D solitons supported by quasi-two-dimensional or fully dimensional lattice potentials.

PACS number(s): 03.75.Lm, 03.75.Kk, 05.45.Yv

Creation of multidimensional solitons built of nonlinear light or matter waves is a great challenge to the experiment. The current situation in this field is summarized in a recent review [1]. The only real example of a quasi-two-dimensional (quasi-2D) spatiotemporal soliton in optics was one created in a $\chi^{(2)}$ (quadratically nonlinear) crystal [2]; it could not be made fully three dimensional (3D), as one transverse direction was reserved to implement the technique of tilted wave fronts, by means of which sufficiently strong artificial dispersion was induced in the medium.

While the experimental situation in optics remains difficult [1], possibilities for the creation of multidimensional solitons are also offered by Bose-Einstein condensates (BECs) with attractive interactions between atoms. In an effectively one-dimensional (1D) condensate of ^{7}Li, single solitons and soliton clusters were successfully created [3]. In the 2D and 3D situations, the self-focusing cubic nonlinearity induced by the attractive interactions leads, respectively, to weak and strong collapse, as predicted by the corresponding Gross-Pitaevskii equation (GPE) [alias the nonlinear Schrödinger (NLS) equation] [4], and demonstrated experimentally in the BEC [5]. However, a spatially periodic potential in the form of an optical lattice (OL), created as an interference pattern by coherent laser beams illuminating the condensate, can stabilize the multidimensional solitons in the self-attractive BEC. For the 2D case, this was first predicted in Refs. [6,7]; moreover, it was also demonstrated [8] that 2D solitons may be stable in the presence of a quasi-1D periodic potential (one that does not depend on the second spatial coordinate). Three-dimensional solitons supported by the 3D OL were reported too [6]. The form of the soliton was predicted by the variational approximation (VA), which was used, as an initial guess, to generate several examples of stable 3D solitons in direct simulations, including "single-cell" and "multicell" ones, that are essentially confined to one or several cells of the OL, respectively. Further, in Refs. [8,9] it was independently demonstrated that stable 3D solitons can also be supported by the low-dimensional, i.e., quasi-2D, lattice potential (however, the quasi-1D potential cannot stabilize 3D solitons [8], unless it is combined with periodic alternation of the nonlinearity sign, which may be provided by the Feshbach resonance in ac magnetic field [10]). In particular, the VA predicts that the 3D solitons in the quasi-2D lattice exist at all values of the norm (number of atoms) N and OL strength p, but are stable only for p exceeding a certain critical value p_{cr}, in an interval of the width $\Delta N_{stab}^{(3D)} \sim (p-p_{cr})^{1/2}$ in a vicinity of a finite value N_{cr} of the norm [8] [the stability was predicted on the basis of the Vakhitov-Kolokolov (VK) [11] criterion].

Except for a few examples reported in Ref. [6], no systematic investigation of the existence, stability, and robustness of 3D BEC solitons in the 3D lattice potential has been performed yet. The objective of the present work is to report basic results for this problem.

The GPE provides for the description of the BEC dynamics in terms of the mean-field single-atom wave function $\psi(x,y,z,t)$ [12]. The normalized form of this equation for a self-attractive condensate trapped in the 3D potential $-V(x,y,z)$ is well known [13],

$$i\frac{\partial\psi}{\partial t} = -\frac{1}{2}\left(\frac{\partial^2\psi}{\partial x^2} + \frac{\partial^2\psi}{\partial y^2} + \frac{\partial^2\psi}{\partial z^2}\right) - |\psi|^2\psi - V(x,y,z)\psi. \quad (1)$$

Generally, $V(x,y,z)$ contains terms accounting for the confining parabolic trap (magnetic and/or optical) and the periodic potential of the OL. Being interested in the localized solutions, occupying a few cells of the lattice, we disregard the parabolic potential and set $V(x,y,z) = p[\cos(4x) + \cos(4y) + \cos(4z)]$, where the OL period is normalized to be $\pi/2$, and the OL strength p is defined to be positive. Besides
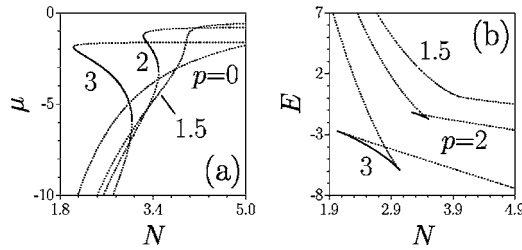
FIG. 1. The chemical potential μ (a) and the energy E (b) of the 3D solitons vs their norm N for different values of the lattice strength p. Full and dotted lines depict stable and unstable solitons, respectively.

FIG. 2. (Color online) The soliton family in terms of the dependence $E=E(\mu,N)$, and its projections on the planes (E,μ), (E,N), and (μ,N) for (a) $p=0$ and (b) $p=3$.

the above-mentioned norm, $N=\iiint|\psi(x,y,z)|^2 dxdydz$, Eq. (1) conserves the energy E [13]. Stationary soliton solutions have the form $\psi(x,y,z,t)=w(x,y,z)\exp(-i\mu t)$, with a real function w and chemical potential μ. We looked for the function $w(x,y,z)$ by means of the known method of the propagation in imaginary time [14]. It was implemented, using the Crank-Nicholson scheme, with the nonlinear finite-difference equations solved by means of the Picard iteration method, and the resulting linear system handled with the help of the Gauss-Seidel iterative procedure. To achieve good convergence, we typically needed six Picard iterations and six Gauss-Seidel iterations. We used equal transverse grid stepsizes, $\Delta x=\Delta y=\Delta z\equiv h$, and a mesh of $361\times361\times361$ points was usually employed. The convergence to a stationary state occurred after 4×10^3–5×10^4 steps of the evolution in imaginary time, typical transverse-grid and time stepsizes being $h=0.02$ and $\Delta t=0.0003$, respectively, for narrow solitons, whereas for broad ones it was enough to take $h=0.07$ and $\Delta t=0.004$.

One can derive a relationship between the norm N, chemical potential μ, real wave function w, and energy E of the stationary solution: $E=\mu N+\frac{1}{2}\iiint w^4(x,y,z)dxdydz$. It can be used to determine the chemical potential μ, once the field profile w is known. This exact relation was also used for verification of accuracy of the numerically found stationary solutions. Notice that, for stationary solitons of the NLS equation in the free 3D space [with $V=0$ in Eq. (1)], the following relations between μ, N, and E are known: $\mu(N)=-CN^{-2}$, $E(N)=CN^{-1}$, $C\approx44.5$ [15,16] (a corollary of this is $d\mu/dN>0$, which immediately shows that these free-space solitons are *always unstable*, as the VK stability criterion requires exactly the opposite, $d\mu/dN<0$).

In Figs. 1(a) and 1(b) we plot the dependences $\mu=\mu(N)$ and $E=E(N)$ for the numerically found family of 3D solitons in the present model. It is seen that, in the presence of the 3D OL, the localized states exist only for μ smaller than some maximum value, $\mu_{\max}(p)$; in fact, it corresponds to the edge of the *band gap* in the spectrum of the linearized equation (1). At values of μ that do not belong to the band gap, no soliton is possible [15]. We note that $\mu_{\max}(p)$ decreases with the increase of the lattice strength p, see Fig. 1(a) [for the 3D NLS equation in free space $(p=0)$, one has $\mu_{\max}(0)=0$]. Remarkably, for sufficiently large values of the lattice strength p, the $E(N)$ curves in Fig. 1(b) feature *two cusps*, instead of a single one, as in most other 2D and 3D Hamiltonian mod-
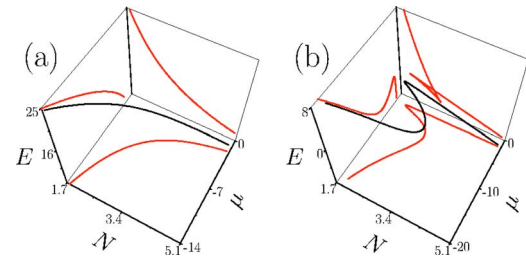
els. Examples of the usefulness of the energy versus norm diagrams (or Hamiltonian versus power diagrams, in the context of spatial optical solitons) in the analysis of the existence and stability of solitons can be found in Ref. [16]. To check the soliton's stability by direct propagation simulations we used the standard Crank-Nicholson discretization scheme with $121\times121\times121$ points in the coordinates x,y,z, and spatial and time stepsizes $0.019\leq h\leq0.073$ and $0.00045\leq\Delta t\leq0.004$ (depending on the soliton's size). The validity of the VK stability criterion was checked by performing direct propagation simulations; the step in the soliton's parameter was $\Delta\mu=0.08$. Thus, we have found stable 3D solitons, in a finite interval of the values of N, if the OL strength p exceeds a threshold value p_{cr}: as seen from Fig. 1, p_{cr} itself is located between $p=1.5$ and $p=2$. Further, Fig. 2 displays an integrated characteristic of the soliton family—the dependence $E=E(\mu,N)$—together with the corresponding projections onto the three planes (E,μ), (E,N), and (μ,N), for two different values of the lattice strength, $p=0$ and $p=3$. In the latter case [in Fig. 2(b)], we notice the *nonmonotonic* behavior of the three projected curves for $p=3$ (above the stability threshold) and the *swallowtail loop* in the energy versus norm diagram. Although this pattern is one of generic possibilities known in the catastrophe theory, it rarely occurs in physical models (applications of the catastrophe theory to the soliton-stability problem were reviewed in Ref. [17]).

It is noteworthy that the qualitative features of the stability picture for the 3D solitons are essentially the same as found earlier in an approximate analytical form by means of the VA [8], and in the numerical form as well [8,9], for 3D solitons supported by the low-dimensional (quasi-2D) lattice: a narrow stability interval ΔN appears in a vicinity of a finite critical value N_{cr}, when the lattice strength p exceeds a finite minimum value p_{cr}. Remarkably, the swallowtail loop was also identified as a characteristic feature of the family of stable 3D solitons supported by 2D harmonic lattices [9]. It is relevant to compare the stability picture for the 3D solitons supported by a fully dimensional OL with that for 2D solitons supported by an OL (that may be either a low-dimensional quasi-1D lattice, or the full 2D one) [6,8,18]: in that case stable solitons appear at *arbitrarily small* values of the lattice strength, and their stability interval extends, in terms of N, up to a maximum ("cutoff") value at which the 2D solitons exist (the latter is actually the norm of the *Townes soliton*, i.e., a soliton of the free-space 2D NLS equation [4]). Thus, we conclude that all the above features, viz.,
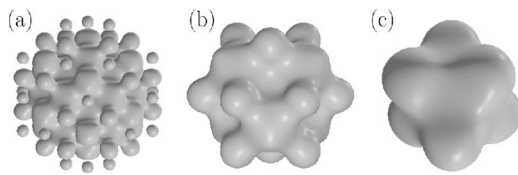
FIG. 3. Isosurface plots of (a) unstable and (b and c) stable 3D solitons. Here $p=3$; (a) $N=2.4$, $A=1.8$, (b) $N=2.04$, $A=2.2$, and (c) $N=2.4$, $A=3$.

the existence of stability threshold p_{cr}, the (small) stability interval ΔN_{stab} for $p > p_{cr}$, and the typical swallowtail pattern in the dependence $E=E(N)$, are generic to 3D solitons supported by lattice potentials, and distinguish them from 2D solitons.

Shapes of both unstable and stable solitons are shown in Fig. 3, through their isosurface plots for a typical value of the lattice strength parameter, $p=3$. An unstable low-amplitude 3D soliton [with $A \equiv w(0,0,0)=1.8$], found for the value of the chemical potential μ close to the band-gap edge, is displayed in Fig. 3(a). This soliton is broad, occupying many lattice cells. Typical *stable* solitons, with medium ($A=2.2$) and high ($A=3$) amplitude, are shown in Figs. 3(b) and 3(c), respectively. Notice that the unstable soliton in Fig. 3(a) and its stable counterpart in Fig. 3(c) have *equal values of the norm*, $N=2.4$. The intermediate stable soliton in Fig. 3(b) has a smaller norm ($N=2.04$), which is very close to the limit value corresponding to the first cuspidal point in the dependence $E=E(N)$ [see the curve pertaining to $p=3$ in Fig. 1(b)]. Figure 4 additionally shows integrated views along the z axis of the isosurface plots displayed in Fig. 3. This figure illustrates the fact that low-amplitude solitons spread to many lattice cells, whereas high-amplitude solitons occupy only a few cells.

An important issue for these 3D solitons is occurrence of the collapse (recall that the 3D collapse in the NLS/GPE is strong, contrary to the weak 2D collapse [4]). We expect that solitons on the stable branch are able to withstand small perturbations without collapse, whereas linearly unstable solitons would either collapse, or reshape themselves into time-periodic breathers, or decay into "radiation" (quasi-linear Bloch waves), depending on the type and strength of the perturbation. In order to verify these expectations, we simulated the evolution of the solitons under small perturbations, taking the initial condition as $\psi(t=0)=w(x,y,z)(1+\epsilon\rho)$, where ϵ is a small amplitude of the perturbation, and ρ is taken either as a random number from the interval $[-0.5,0.5]$ (stochastic perturbation) or as $\rho \equiv 1$ (uniform perturbation). We have checked that the solitons belonging to the VK-stable segments of the curve $\mu=\mu(N)$ are indeed
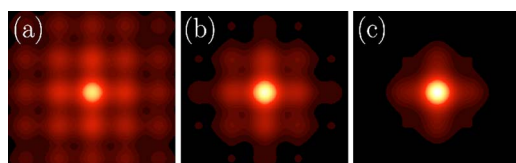

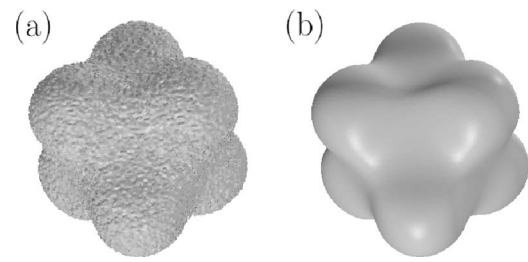FIG. 4. (Color online) Integrated through views along the z axis of the solitons shown in Fig. 3.

FIG. 5. Isosurface plots showing self-cleaning of a stable soliton corresponding to $p=3$ and $N=2.4$, initially perturbed by white noise. (a) Input at $t=0$; (b) output at $t=50$.

stable against small perturbations. To illustrate this result, Fig. 5 shows an example of a stable soliton which persists after the application of the stochastic perturbation with $\epsilon=0.1$: in the course of the evolution, the soliton's amplitude slightly oscillates, with no trend to collapse or breakup. This and many other simulations clearly show that the linearly stable solitons are also *nonlinearly stable* objects. For linearly unstable solitons, the simulations reveal the following scenarios of the instability development: (i) Low-amplitude solitons decay into linear waves under stochastic perturbations, or under uniform ones that reduce the soliton's norm, i.e., perturbations with $\rho \equiv 1$ and $\epsilon < 0$; this case is illustrated by Fig. 6 for a typical situation. (ii) The same unstable soliton, but under uniform perturbations with $\rho \equiv 1$ and $\epsilon > 0$ (that make its norm larger), reshapes itself into a time-periodic breather. (iii) An unstable high-amplitude soliton collapses if it is perturbed by the uniform perturbation that increases its norm.

In conclusion, we have found one-parameter soliton families of the 3D nonlinear Schrödinger/Gross-Pitaevskii equation with self-focusing nonlinearity and 3D lattice potential, and explored their stability. Comparing the results with recently published findings for stable 3D solitons in the quasi-2D lattice potential, and with (very different) results for 2D solitons supported by the quasi-1D or full 2D lattice, we were able to identify generic features that distinguish the stable 3D solitons: a finite stability threshold p_{cr} in terms of the lattice strength p, a finite stability interval ΔN in terms of the soliton's norm N, and the swallowtail shape of the energy versus norm dependence. The 3D solitons investigated here can be created in BEC, most plausibly, using [7]Li loaded into a 3D optical lattice, with the spatial period $\Lambda \sim 0.5\ \mu$m. Then, undoing normalizations that cast the GPE into the rescaled form (1), it is easy to find that the actual number of atoms N_{phys} is related to the solution norm by N_{phys}
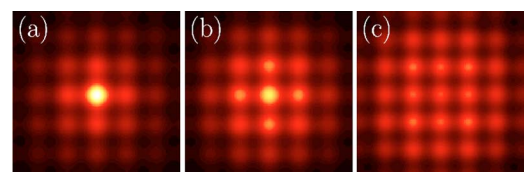

FIG. 6. (Color online) Integrated through views along the z axis of an unstable soliton that decays due to a uniform norm-reducing perturbation with $\epsilon=0.01$, for $p=3$. (a) $t=0$, $A=1.78$; (b) $t=50$, $A=0.650\ 5$; (c) $t=70$, $A=0.207\ 5$.

RAPID COMMUNICATIONS

$=(2\pi^2|a|)^{-1}\Lambda N$, where a is the scattering length of the atomic collisions. For ^{7}Li, $a=-1.45$ nm, which yields the minimum number of atoms necessary for the formation of stable solitons, that corresponds to $N_{cr}\approx 3.5$ in Fig. 1: $N_{phys}^{(min)}\approx 60$ (note that it corresponds to the density $\sim 5 \times 10^{14}$ cm^{-3}, which is quite a typical value for BEC). The strength ε of the OL, chemical potential, and energy in physical units are related to their normalized strength counterparts as $\varepsilon=(1/8)E_{rec}p$, $\mu_{phys}=(1/4)E_{rec}\mu$, $E_{phys}=[\hbar^2/(8|a|\Lambda m)]E\equiv\{\Lambda/[(4\pi)^2|a|]\}E_{rec}E$, where

$E_{rec}=(2/m)(\pi\hbar/\Lambda)^2\approx 7.5\times 10^{-29}$ J is the recoil energy in the lattice. Thus, near the soliton-stability threshold, we get $\varepsilon\approx 0.25E_{rec}$, $\mu_{phys}\approx -E_{rec}$, and $E_{phys}\approx -6E_{rec}$.

[1] B. A. Malomed, D. Mihalache, F. Wise, and L. Torner, J. Opt. B: Quantum Semiclassical Opt. **7**, R53 (2005).

[2] X. Liu, L. J. Qian, and F. W. Wise, Phys. Rev. Lett. **82**, 4631 (1999); X. Liu, K. Beckwitt, and F. Wise, Phys. Rev. E **62**, 1328 (2000).

[3] K. E. Strecker *et al.*, Nature (London) **417**, 150 (2002); L. Khaykovich *et al.*, Science **296**, 1290 (2002).

[4] L. Bergé, Phys. Rep. **303**, 260 (1998).

[5] E. A. Donley *et al.*, Nature (London) **412**, 295 (2001).

[6] B. B. Baizakov, B. A. Malomed, and M. Salerno, Europhys. Lett. **63**, 642 (2003).

[7] J. Yang and Z. H. Musslimani, Opt. Lett. **28**, 2094 (2003).

[8] B. B. Baizakov, B. A. Malomed, and M. Salerno, Phys. Rev. A **70**, 053613 (2004).

[9] D. Mihalache *et al.*, Phys. Rev. E **70**, 055603(R) (2004); Phys. Rev. Lett. **95**, 023902 (2005).

[10] M. Trippenbach, M. Matuszewski, and B. A. Malomed, Europhys. Lett. **70**, 8 (2005).

[11] M. G. Vakhitov and A. A. Kolokolov, Izv. Vuz. Radiofiz. **16**, 1020 (1973).[Sov. J. Radiophys. Quantum Electron. **16**, 783 (1973)].

[12] E. P. Gross, Nuovo Cimento **20**, 454 (1961); L. P. Pitaevskii, Sov. Phys. JETP **13**, 451 (1961).

[13] F. Dalfovo *et al.*, Rev. Mod. Phys. **71**, 463 (1999).

[14] M. L. Chiofalo, S. Succi, and M. P. Tosi, Phys. Rev. E **62**, 7438 (2000).

[15] Yu. S. Kivshar and G. P. Agrawal, *Optical Solitons: From Fibers to Photonic Crystals* (Academic, San Diego, 2003).

[16] N. N. Akhmediev and A. Ankiewicz, *Solitons: Nonlinear Pulses and Beams* (Chapman and Hall, London, 1997).

[17] F. V. Kusmartsev, Phys. Rep. **183**, 1 (1989).

[18] N. K. Efremidis *et al.*, Phys. Rev. Lett. **91**, 213906 (2003).